Preprints.org

Article

Not peer-reviewed version

Concurrent Multi-Beam Digital Pre-Distortion Using FFT Beamforming and Virtual Arrays

Björn Langborn * , Christian Fager , Rui Hou , Thomas Eriksson

Posted Date: 9 February 2026

doi: 10.20944/preprints202602.0713.v1

Keywords: digital predistortion; DPD; virtual array; power amplifier; PA; MIMO; multi-beam; beam domain

Preprints.org is a free multidisciplinary platform providing preprint service that is dedicated to making early versions of research outputs permanently available and citable. Preprints posted at Preprints.org appear in Web of Science, Crossref, Google Scholar, Scilit, Europe PMC.

Copyright: This open access article is published under a Creative Commons CC BY 4.0 license, which permit the free download, distribution, and reuse, provided that the author and preprint are cited in any reuse.

Preprints.org (www.preprints.org) | NOT PEER-REVIEWED | Posted: 9 February 2026
doi:10.20944/preprints202602.0713.v1

Disclaimer/Publisher's Note: The statements, opinions, and data contained in all publications are solely those of the individual author(s) and contributor(s) and not of MDPI and/or the editor(s). MDPI and/or the editor(s) disclaim responsibility for any injury to people or property resulting from any ideas, methods, instructions, or products referred to in the content.

Article

Concurrent Multi-Beam Digital Pre-Distortion Using FFT Beamforming and Virtual Arrays

Björn Langborn [1,*], Christian Fager [2], Rui Hou [3] and Thomas Eriksson [1]

1 Department of Electrical Engineering, Chalmers University of Technology, Sweden
2 Department of Microtechnology and Nanoscience, Chalmers University of Technology, Sweden
3 Department of Microtechnology and Nanoscience, Chalmers University of Technology, Sweden and Ericsson AB, Stockholm, Sweden
* Correspondence: langborn@chalmers.se

Abstract

A digital pre-distortion (DPD) scheme for concurrent multi-beam transmission in fully digital multiple-input, multiple-output (MIMO) systems, using fast Fourier transform (FFT) beamforming and so-called virtual array processing, is proposed. In a MIMO array with nonlinear power amplifiers (PAs), transmitting multiple beams concurrently yields intermodulation products that end up in both user and non-user directions. In the setting with few users in a large array, the array dimension will typically be much larger than the number of generated intermodulation products. At the same time, linearization per-PA is excessively costly for large arrays. This work shows that is instead possible to linearize the system by producing predistorted user beams, and non-user intermodulation products, through DPD processing in a virtual array, of a much smaller dimension than the physical array. Theoretical derivations and simulation examples show how this approach can lead to manyfold reductions in DPD complexity.

Keywords: digital predistortion; DPD; virtual array; power amplifier; PA; MIMO; multi-beam; beam domain

---

1. Introduction

Multi-antenna transmitters offer the possibility to spatially direct multiple beams[1] concurrently, which is of interest for many applications. For communication, it allows base stations to serve multiple users in different locations concurrently. For localization and sensing, utilizing multi-beam schemes can improve localization accuracy [1]. To utilize these possibilities fully in future radio systems, the number of transmit branches is expected to increase dramatically. Simultaneously, operating PAs with as high efficiency as possible always comes with a compromise in their linearity. However, generating distortion due to non-linear operation is problematic for multiple reasons. Firstly, distortion will be emitted in-band in the directions of the users, deteriorating communication link quality. Secondly, distortion will be generated both in-band and out-of-band into non-user directions and can interfere with other systems. As such, non-linear distortion must be considered to fulfill transmission requirements. To this end, DPD is widely adopted.

To linearize multi-antenna transmitters, numerous schemes have been proposed, as detailed in Section 1.1, in which this paper will focus on fully digital beamforming. Some works have been either concerned with cancelling distortion specifically in user directions [2,3], or cancelling distortion going in all directions from the transmitter when one main beam is considered [4]. Recent, state-of-the-art research has also considered distortion cancellation in different beam directions whilst concurrently transmitting multiple beams, so-called beam domain DPD (BD-DPD) [5,6].

BD-DPD for multi-beam linearization is similar to multidimensional DPDs from the concurrent multi-band setting, such as 2D and 3D-DPD [7–10]. These linearization approaches take multiple user

1 The concept of a beam in this paper will sometimes be used interchangeably with a precoded data stream, generalizing statements from line-of-sight to other channel conditions.

© 2025 by the author(s). Distributed under a Creative Commons CC BY license.

Preprints.org (www.preprints.org) | NOT PEER-REVIEWED | Posted: 9 February 2026 doi:10.20944/preprints202602.0713.v1

data streams as input to a DPD, and combines the streams to generate a set of multi-dimensional basis functions. As such they suffer the drawback of a drastically increasing number of multi-dimensional basis functions as the number of user streams increase. One alternative approach to this in the multi-band setting is frequency relocation [11], which involves relocating bands to lie closer in frequency, and generating all the necessary basis functions for linearization through a single nonlinearity before inverse frequency relocation. No similar technique to this exists in the multi-beam setting, to the authors' best knowledge.

1.1. Previous Work

Handling distortion emitted from multi-input, multi-output (MIMO) transmitters can be done differently depending on system requirements, available resources and number of users to be served simultaneously. Previous work within two approaches for considering the emitted distortion will be briefly outlined here.

A first approach to handling nonlinear distortion in MIMO transmitter systems, done in e.g. [12], is to make distortion nulls in the beamforming pattern in specific directions. However, in [12] a single-user scenario is studied, referring to [13] for the observation that in a setting with either many beams and/or multiple channel taps, the distortion tends to be quite isotropically transmitted. This glosses over the case when e.g. there are multiple, but few, beams in relation to the array size. Additionally, a nullforming approach can prevent distortion from being transmitted in specific directions, but it will not be able to prevent distortion from being generated at the PA outputs and subsequently transmitted in many directions. For that, distortion compensation is needed.

A second approach to handling nonlinear distortion is thereby through linearization. In a fully digital beamforming MIMO system, the most straight-forward approach to linearization is adopting one DPD per PA in the transmitter chain. However, whilst likely to work well for linearization it is quite costly, both economically and in terms of energy consumption as well as in complexity, as the number of transmit branches increases. To address this, researchers have suggested alternative solutions.

For a MIMO transmitter with a single beam, so-called full-angle DPD [4] has been proposed. Here, instead of linearizing L PAs with L equal-size DPDs, it is proposed to use a common DPD for all branches and to perform only minor tuning in the branches to consider branch-wise variations. It is shown to perform well, and to be able to effectively cancel distortion from the transmitter. Worth noting in this approach is that it still requires tuning for all the branches but one, that is used as reference. From their results it can be seen that the tuning boxes are not insignificant in size, as their common DPD had 21 coefficients whilst the tuning boxes each had 3-10 coefficients. Lastly, the DPD scheme considers only a single beam, whilst it in practice is of great interest to transmit multiple beams concurrently.

Several works addressing the topic of multi-beam linearization are available. In [3], the objective is set to cancel inter-user distortion arising due to concurrent multi-beam operation, which is verified to work well for two users. Similarly, a technique for cancelling inter-user distortion is proposed and verified for three users in [14]. However, none of these works consider the distortion in non-user directions.

In [5] BD-DPD was adopted to perform linearization prior to the beamformer, using the user data streams rather than the precoded data streams going to each PA. With this approach, the DPD complexity scales in relation to the number of users K and user stream intermodulation products, rather than the number of antennas L. For $K \ll L$, this can yield large complexity savings. As aforementioned though, in similarity to 2D- and 3D-DPD for multiband signals, the number of intermodulation products scales drastically with larger K. Furthermore, it results in multi-dimensional bases, e.g. basis functions of the form $x_1 x_2 x_3^*$. This is important to note, as for how the DPD scheme can be adapted to a look-up table (LUT) implementation, which is often made in practice to reduce arithmetic computations at the expense of memory. Adaptation of multi-dimensional basis functions to LUTs requires multi-dimensional tables, which both increases memory use but also computational cost for interpolation and extrapolation operations. This is exemplified in [15] for concurrent dual-band transmission. Lastly, BD-DPD assumes equal PAs across branches. In the presence of PA variations, the performance of BD-DPD is expected to deteriorate.

© 2025 by the author(s). Distributed under a Creative Commons CC BY license.

Preprints.org (www.preprints.org) | NOT PEER-REVIEWED | Posted: 9 February 2026 doi:10.20944/preprints202602.0713.v1

1.2. Key Contributions and Paper Organization

In this paper, a novel approach to DPD processing using a so-called virtual array is proposed, for concurrent multi-beam linearization. In essence, the virtual array processing involves passing user streams through a low-dimensional virtual transmit array structure, and a virtual channel, whose operation is dependent on that of the actual transmit array. In the actual transmit array, L branches with nonlinear PAs will generate intermodulation (IM) distortion that will be emitted over-the-air (OTA) in both user and non-user directions when the signals are passed through antennae. In the virtual array instead, L_v branches with nonlinear DPDs aim to produce IM terms to cancel out those generated in the real array, though with much fewer branches, $L_v \ll L$. It has similarities to how previous work performed dimensionality reduction for the multi-band setting, utilizing frequency domain sparseness, via frequency relocation [11] or non-uniform downsampling [16]. However, this work performs dimensionality reduction for the multi-beam setting, utilizing so-called beam domain sparseness.

The specific contributions of this paper are as follows:

- A novel approach to multi-beam DPD for MIMO transmitters, performing DPD in a small virtual antenna space, is proposed and exemplified. It is shown how such an approach can lead to manyfold reductions in complexity.
- Practical considerations in implementing the proposed scheme are accounted for, through simulation and discussion, considering multi-user cases, different channels and LUT implementation.
- Simulation results verify the theoretical findings, and show the applicability of the proposed scheme, and how the DPD scales in computational complexity in relation to the number of users.

To lead up to those contributions, the paper is organized as follows. The assumed system model description is expanded upon in Section 2. Firstly, in Subsection 2.1, the model description is expanded upon in order to comprehend how distortion is spatially distributed in the beam domain during concurrent multi-beam operation. After that, in Subsection 2.2, Fast-Fourier Transform (FFT) beamforming is described. This is followed in Section 3 by an example, where the orthogonality of FFT beamforming highlights the sparsity of the beam domain after over-the-air (OTA) transmission. Section 4 goes on to describe how processing in a virtual array, smaller than the actual physical one, can produce the same linearization signals as per-PA (PP) DPD but at a lower computational cost. Lastly, numerical simulation results are presented in Section 5 to verify the proposed approach, alongside a conclusion in Section 6.

2. System Modeling

The system modeling of this work focuses on a discrete time-domain, baseband description of concurrent multi-beam transmission in a fully digital multi-branch transmitter setting. Firstly by detailing how intermodulation products, arising from nonlinear PAs, can be understood in such a description, and then related to FFT-beamforming as to motivate the suitability of the proposed approach.

Concepts referred to in this work is the beam domain, and the antenna space. The beam domain is a domain encompassing signals that have propagated through a channel and, as a result of beamforming, have formed beams. In Figure 1, this domain is indicated with the red and orange beams, that are observed over-the-air in different directions as signals $y^{(1)}, ..., y^{(Q)}$. The user streams $x_1, ..., x_K$ are contained in some of these beams, whilst others contain only IM terms. In contrast, the antenna space refers to the signals on the different transmit branches, prior to channel propagation. In Figure 1, the antenna space encompasses the signals $u_1, ..., u_L$, $z_1, ..., z_L$ but also $f_{\mathrm{PA},1}(z_1), ..., f_{\mathrm{PA},L}(z_L)$. The spaces are as such related through multiplication with a channel or beamforming matrix. For a channel $\boldsymbol{H} \in \mathcal{C}^{Q\times L}$, a signal $\boldsymbol{z} \in \mathcal{C}^{L\times N}$ in the antenna space, where N is the number of baseband data samples, the corresponding beam-domain signal is $\boldsymbol{Y} = \boldsymbol{H}\boldsymbol{z} \in \mathcal{C}^{Q\times N}$. This relation is of particular interest when $Q = L$, and $\boldsymbol{H}$ is an orthogonal matrix, as will be later seen in the subsection on Fast-fourier transform beamforming. Additionally, whilst this paper initially expands upon the relation between the antenna space and beam domain in the context of line-of-sight (LOS) channels, it is later addressed for non-LOS conditions as well.

© 2025 by the author(s). Distributed under a Creative Commons CC BY license.

Preprints.org (www.preprints.org) | NOT PEER-REVIEWED | Posted: 9 February 2026 doi:10.20944/preprints202602.0713.v1

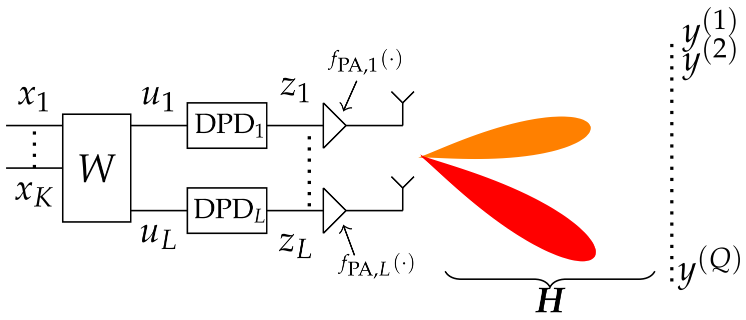

Figure 1. Concurrent multi-beam transmitter schematic of K user data streams, beamformed by $\boldsymbol{W}$, passed through DPDs, transmitted through PAs on L antenna branches and observed in Q directions.

2.1. Concurrent Transmission of Multiple Beams

Consider the schematic setup of Figure 1, but start by letting the DPDs be bypassed such that $\boldsymbol{z}_l = \boldsymbol{u}_l$, $l = 1, \ldots, L$. In this setup, the beamformer $\boldsymbol{W}$ is formed to direct user streams $x_1, \ldots, x_K$ to directions $1, \ldots, Q$ in matrix form as

$$\boldsymbol{W} = \left[\boldsymbol{w}^{(1)} \ \ldots \ \boldsymbol{w}^{(K)} \right], \tag{1}$$

with $||\boldsymbol{w}^{(k)}||_2 = 1$, yielding PA input signals

$$\begin{bmatrix} z_1 \\ z_2 \\ \vdots \\ z_L \end{bmatrix} = [\boldsymbol{w}^{(1)}, \ldots, \boldsymbol{w}^{(K)}] \begin{bmatrix} x_1 \\ x_2 \\ \vdots \\ x_K \end{bmatrix}. \tag{2}$$

Alternatively, the signal z_l passed to PA l can be written as

$$z_l = w_l^{(1)} x_1 + \ldots + w_l^{(K)} x_K \,. \tag{3}$$

Now, it is well-known that an infinite Volterra series can model any non-linear function, such as PAs. For practical application however, finite truncations of the Volterra series are instead used frequently. For qualitative analysis here, consider simply a third order polynomial baseband PA model as

$$f_{\mathrm{PA},l}(z_l) = c_{1,l} z_l + c_{3,l} z_l |z_l|^2 \,. \tag{4}$$

where $f_{\mathrm{PA},l}$ refers to the non-linear function of the PA in branch l, and $c_{1,l}, c_{3,l}$ are modeling coefficients. Then, inserting (3) into (4), this yields

$$\begin{aligned} f_{\mathrm{PA},l}(z_l) = {} & c_{1,l}(w_l^{(1)} x_1 + \ldots + w_l^{(K)} x_K) + \\ & c_{3,l}(w_l^{(1)} x_1 + \ldots + w_l^{(K)} x_K) |w_l^{(1)} x_1 + \ldots + w_l^{(K)} x_K|^2 \\ = {} & c_{1,l}(w_l^{(1)} x_1 + \ldots + w_l^{(K)} x_K) + \\ & c_{3,l}(w_l^{(1)} w_l^{(1)} w_l^{(1)*} x_1 |x_1|^2 + \\ & \quad w_l^{(1)} w_l^{(2)} w_l^{(2)*} x_1 |x_2|^2 + \\ & \quad w_l^{(1)} w_l^{(1)} w_l^{(2)*} x_1^2 x_2^* + \ldots) \,. \end{aligned} \tag{5}$$

First, assume that all PAs are equal, such that $c_{1,l}$ and $c_{3,l}$ are the same for each branch l. Then, let each PA output propagate through a channel vector $\boldsymbol{h}_l = \left[h_l^{(1)} \ \ldots \ h_l^{(Q)} \right]$ from branch l to OTA location q, as

$$y^{(q)} = \left[h_1^{(q)} \ \ldots \ h_L^{(q)} \right] \left[f_{\mathrm{PA},1}(z_1) \ \ldots \ f_{\mathrm{PA},L}(z_L) \right]^T. \tag{6}$$

© 2025 by the author(s). Distributed under a Creative Commons CC BY license.

Preprints.org (www.preprints.org) | NOT PEER-REVIEWED | Posted: 9 February 2026 doi:10.20944/preprints202602.0713.v1

Considering the first-order, linear terms

$$\begin{aligned} y_{1\text{st}}^{(q)} &= h_1^{(q)} c_1 (w_1^{(1)} x_1 + \ldots + w_1^{(K)} x_K) + \ldots \\ &\quad + h_L^{(q)} c_1 (w_L^{(1)} x_1 + \ldots + w_L^{(K)} x_K) \,. \end{aligned} \tag{7}$$

Then it is known from beamforming theory that if x_1 is to go in direction (q), then beamforming weights can be chosen such that $w_l^{(1)} = (h_l^{(q)})^*$. This yields constructive interference $c_1 \sum h_l^{(q)} w_l^{(1)} = c_1 L$. Then, studying the third order terms in (5), it can be seen since $w_l^{(1)} w_l^{(1)*}, w_l^{(2)} w_l^{(2)*}$ will be real constants that $x_1|x_1|^2$ and $x_1|x_2|^2$ will also go in direction (q). However, the summation of the IM products last listed in (5), $c_3 \sum_l h_l^{(q)} w_l^{(1)} w_l^{(1)} w_l^{(2)*}$ typically has constructive interference in a direction other than (q). Generally, it can be seen that the terms of the form $\boldsymbol{w}^{(i)} \boldsymbol{w}^{(j)} \boldsymbol{w}^{(k)*}$, where $k \neq i, j$, will give rise to new beam directions of constructive interference, that are referred to as off-beams.

Two interesting observations can be made from (5), still assuming $c_{3,l} = c_3 \,\forall l$. Firstly, the generated off-beam terms and directions can be deterministically computed from the intended transmit directions. Off-beam terms for a static non-linearity of order $P = 3$, and with $K = 2, 3, 4$ concurrent users are listed in Table 1 to exemplify. Secondly, the non-linear products of the input streams are of a different form in the off-beams than for the in-beam. Thus, one needs to be aware of all beam directions and manage to generate the correct IM terms in the respective directions in order to linearize the system. This can readily be understood to grow more complex with more beams.

Table 1. Off-beam terms for static non-linearity of order $P = 3$, and with $K = 2, 3, 4$ concurrent users.

Number of users	**Off-beam terms**	**Number of off-beam terms**
$K = 2$	$x_1 x_1 x_2^*, x_2 x_2 x_1^*$	2
$K = 3$	$x_1 x_1 x_2^*, x_2 x_2 x_1^*, x_1 x_1 x_3^*, x_3 x_3 x_1^*$ $x_2 x_2 x_3^*, x_3 x_3 x_2^*, x_1 x_2 x_3^*, x_1 x_3 x_2^*, x_2 x_3 x_1^*$	9
$K = 4$	$x_1 x_1 x_2^*, x_2 x_2 x_1^*, x_1 x_1 x_3^*, x_3 x_3 x_1^*$ $x_2 x_2 x_3^*, x_3 x_3 x_2^*, x_1 x_2 x_3^*, x_1 x_3 x_2^*,$ $x_2 x_3 x_1^*, x_1^2 x_4^*, x_4^2 x_1^*, x_2^2 x_4^*, x_4^2 x_2^*, x_3^2 x_4^*,$ $x_4^2 x_3^*, x_1 x_2 x_4^*, x_1 x_4 x_2^*, x_2 x_4 x_1^*, x_1 x_3 x_4^*,$ $x_1 x_4 x_3^*, x_3 x_4 x_1^*, x_2 x_3 x_4^*, x_2 x_4 x_3^*, x_3 x_4 x_2^*$	24

2.2. Fast-Fourier Transform Beamforming

FFT-beamforming is one common way to computationally efficiently limit the beamforming matrix to an orthogonal set of beam directions, by first defining

$$\omega = e^{-j2\pi/L} \,. \tag{8}$$

Then a one-dimensional discrete Fourier transform (DFT) beamformer matrix can be formulated as

$$\mathbf{W}_{\text{DFT}} = \frac{1}{\sqrt{L}} \begin{bmatrix} 1 & 1 & 1 & \ldots \\ 1 & \omega & \omega^2 & \ldots \\ 1 & \omega^2 & \omega^4 & \ldots \\ \vdots & \vdots & \vdots & \vdots \end{bmatrix} = \frac{1}{\sqrt{L}} \left[\omega^{(b_1)} \;\; \omega^{(b_2)} \;\; \omega^{(b_3)} \;\; \ldots \right], \tag{9}$$

where $b_i \in [1, L]$ are beam indices, indexing the beams on the DFT-beamgrid. In implementation though, no matrix multiplication of $\mathbf{W}_{\text{DFT}}$ with data is needed, as would otherwise be indicated by (2). Instead, FFT algorithms can perform this computation at lower complexity.

It is worth to note that when the main beams are limited to a DFT-beamgrid, $b_i \in [1, L]$, the off-beam directions will be restricted to the same beamgrid as well, given equal PAs. Furthermore, extension to two-dimensional beamforming is straightforward, by implementing FFT along both a horizontal and vertical direction, but omitted from the derivations for brevity. All the analysis following in this paper can then be applied to each dimension, horizontal or vertical, separately.

With the system modeling etablished, the following section details how per-PA (PP) DPD produces predistorted streams, and how intermodulation beam placement is affected by aliasing due to the antenna array being finite and discrete.

© 2025 by the author(s). Distributed under a Creative Commons CC BY license.

3. Per-PA DPD

In this section, the processing steps of transmitting K user streams with PP-DPD, as in Figure 1, is detailed with a three-user example. With this example, the sparsity of the problem for larger L is highlighted, in addition to noting an effect that will be referred to as array aliasing.

3.1. Per-PA DPD Example for Three Concurrent Users

Let the antenna array be a linear, one-dimensional array in space, and restrict the beamformer to a DFT-beamgrid. Consider that there are $L = 16$ transmit branches[2], transmitting data x_1, x_2, x_3 to $K = 3$ users in different LOS directions. Being restricted to a DFT-beamgrid, the users can be located at beam indices $\{b_1, b_2, b_3\} \in [1, L]$. To exemplify, let $b_1 = 1, b_2 = 2, b_3 = 5$ and let $\boldsymbol{W}_{\text{DFT}}$ be the DFT beamforming matrix to the user directions, such that

$$\begin{aligned}
\boldsymbol{z} = \boldsymbol{W}\boldsymbol{x} &= \frac{1}{\sqrt{L}}\begin{bmatrix} 1 & 1 & 1 & \dots \\ 1 & \omega & \omega^2 & \dots \\ 1 & \omega^2 & \omega^4 & \dots \\ \vdots & \vdots & \vdots & \vdots \end{bmatrix}\begin{bmatrix} x_1 \\ x_2 \\ 0 \\ 0 \\ x_3 \\ 0 \\ \vdots \end{bmatrix} \\
&= \frac{1}{\sqrt{L}}\begin{bmatrix} x_1+x_2+x_3 \\ x_1+\omega x_2+\omega^4 x_3 \\ x_1+\omega^2 x_2+\omega^8 x_3 \\ \vdots \end{bmatrix} \\
&= \boldsymbol{\omega}^{(b_1)}x_1 + \boldsymbol{\omega}^{(b_2)}x_2 + \boldsymbol{\omega}^{(b_3)}x_3\,.
\end{aligned} \tag{10}$$

Applying the nonlinear DPDs to each of these beamformed data streams, with a third order nonlinearity $f(x) = \theta_1 x + \theta_3 x|x|^2$ as the DPD function, then

$$f(\boldsymbol{W}\boldsymbol{x}) = \underbrace{\begin{bmatrix} \theta_1(x_1+x_2+x_3)+\theta_3(x_1+x_2+x_3)|x_1+x_2+x_3|^2 \\ \theta_1(x_1+\omega x_2+\omega^4 x_3)+\theta_3(x_1+\omega x_2+\omega^4 x_3)|x_1+\omega x_2+\omega^4 x_3|^2 \\ \theta_1(x_1+\omega^2 x_2+\omega^8 x_3)+\theta_3(x_1+\omega^2 x_2+\omega^8 x_3)|x_1+\omega^2 x_2+\omega^8 x_3|^2 \\ \vdots \end{bmatrix}}_{L\times 1}, \tag{11}$$

is obtained. How these signals will be spatially distributed OTA can be seen by transformation to the beam domain, i.e. by simulating a channel $\boldsymbol{H}$ through an inverse Fourier transform. The user streams will then be clearly separated in the beam-domain, like the beams in Figure 1. With the matrix $\boldsymbol{W}_{\text{IDFT}} = L\boldsymbol{W}^*_{\text{DFT}}$, the data streams are

$$L\boldsymbol{W}^*_{\text{DFT}} f(\boldsymbol{W}\boldsymbol{x}) = \begin{bmatrix} \theta_1 x_1+\theta_3 x_1(|x_1|^2+|x_2|^2+|x_3|^2) \\ \theta_1 x_2+\theta_3 x_2(|x_1|^2+|x_2|^2+|x_3|^2) \\ \theta_3 x_2^2 x_1^* \\ \theta_3 x_1 x_3 x_2^* \\ \theta_1 x_3+\theta_3 x_3(|x_1|^2+|x_2|^2+|x_3|^2) \\ \theta_3 x_2 x_3 x_1^* \\ 0 \\ \theta_3 x_3^2 x_2^* \\ \theta_3 x_3^2 x_1^* \\ 0 \\ 0 \\ 0 \\ \theta_3 x_1^2 x_3^* \\ \theta_3 x_1 x_2 x_3^* \\ \theta_3 x_2^2 x_3^* \\ \theta_3 x_1^2 x_2^* \end{bmatrix}. \tag{12}$$

Each entry at a separate index here represents a signal going in a unique beam direction. Two observations are worth note. The first observations is that only 12 out of the 16 entries are non-zero. This is unsurprising, but important, as Table 1 shows that there can only be up to nine off-beam terms going in potentially different directions, in addition to the $K = 3$ user directions, for a third order nonlinearity. This is also true when L is a much larger value. Thus, for large L, there are very few low-order signal components in relation to the array size. As for the second observation, concerning where each signal component ends up on the beam grid, it is detailed in the following subsection.

[2] Whilst $L = 16$ is chosen for these derivations, for simpler equations, the value of L would typically be much larger in practice.

© 2025 by the author(s). Distributed under a Creative Commons CC BY license.

Preprints.org (www.preprints.org) | NOT PEER-REVIEWED | Posted: 9 February 2026 doi:10.20944/preprints202602.0713.v1

3.2. Array Aliasing

In (12), the intermodulation terms end up deterministically at a beam index by summing or subtracting the corresponding term's precoder beam indices. Exemplified, the intermodulation term $(\omega^{(b_2)}x_2)^2(\omega^{(b_1)}x_1)^* = (\omega^{(b_2)}\omega^{(b_2)}\omega^{(b_1)*})x_2^2x_1^*$ indeed produces the intermodulation term $x_2^2x_1^*$ up on beam index $b_2 + b_2 - b_1 = 2 + 2 - 1 = 3$. However, this can not hold for the term $(\omega^{(b_1)}x_1)^2(\omega^{(b_2)}x_2)^*$ as $2b_1 - b_2 = 0 \notin [1, L]$. Instead, this term is aliased back in to the beam grid range $[1, L]$ according to

$$\overline{b_{i_1} + b_{i_2} - b_{i_3}} = b_{i_1} + b_{i_2} - b_{i_3} - L\left\lfloor \frac{b_{i_1} + b_{i_2} - b_{i_3} - 1/2}{L} \right\rfloor, \tag{13}$$

for $\{b_{i_1}, b_{i_2}, b_{i_3}\} \in [1, L]$, $\{i_1, i_2, i_3\} \in [1, ..., K]$. With this in mind, it can be noted that whilst the example of Subsection 3.1 produced 12 uniquely placed data streams of main beam and intermodulation beam data, aliasing can for a different beam configuration $\{b_1, b_2, b_3\}$ end up overlapping intermodulation terms to go in the same beam directions. This will lead to distortion being concentrated in fewer beam directions.

4. Virtual Array DPD

In this section, virtual array DPD (VA-DPD) processing as in Figure 2 is proposed to reduce the complexity compared to applying a DPD per PA. As previously described in Subsection 1.2, the VA-DPD aims to produce predistorted user streams and off-beam IM terms in a low-dimensional virtual array, and use these to linearize the larger, real transmit array. This is done in steps. First, user streams are precoded to the antenna space of a virtual array, by placement on a beamgrid and through an FFT. The beam placement in the virtual array depends on the precoding to be done in the real array, which will be detailed later. Second, nonlinear DPDs are applied to the data in each of the L_v virtual antenna space branches. Third, an IFFT is performed, acting as a channel and to separate user streams and off-beam IM terms in the virtual beam space. Fourth, and last, the predistorted streams that have been generated are precoded to the real array. In the following subsections, the derivations of Section 3.1 will be used as a starting point to give mathematical motivation as to how a smaller, virtual array, in place of the original array, can be used for performing DPD. This is presented first with an example comparison to the per-PA case, followed by presenting special beam configuration cases in which the complexity can be reduced even further, and finally generalizations to more general channels and higher order modeling.

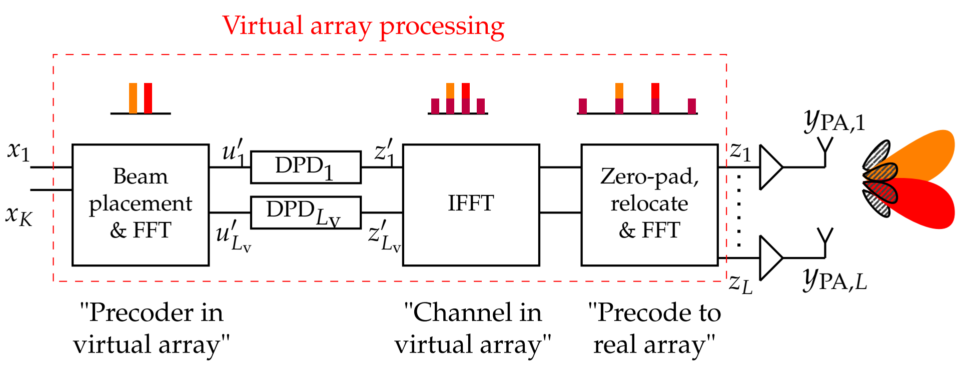

Figure 2. Schematic of DPD using virtual array processing. The bar plots exemplify the beam space representation of beamforming the data streams to beams and induced IM beams. Red and orange correspond to desired user signals, purple to the injected distortion by the DPDs to cancel out the unwanted distortion, shown in striped dark gray. Here, the number of virtual branches L_v can always be made less or equal to the number of antenna branches L.

© 2025 by the author(s). Distributed under a Creative Commons CC BY license.

Preprints.org (www.preprints.org) | NOT PEER-REVIEWED | Posted: 9 February 2026 doi:10.20944/preprints202602.0713.v1

4.1. Virtual Array DPD Example for Three Concurrent Users

Revisiting the example of Subsection 3.1, with $\{b_1, b_2, b_3\} = \{1, 2, 5\}$ but replacing $L = 16$ with $L_\mathrm{v} = 13$ for the derivation, the computation steps are straightforward to compute, ending with

$$L_\mathrm{v}\boldsymbol{W}^*_\mathrm{DFT} = \begin{bmatrix} \theta_1 x_1 + \theta_3 x_1 (|x_1|^2 + |x_2|^2 + |x_3|^2) \\ \theta_1 x_2 + \theta_3 x_2 (|x_1|^2 + |x_2|^2 + |x_3|^2) \\ \theta_3 x_2^2 x_1^* \\ \theta_3 x_1 x_3 x_2^* \\ \theta_1 x_3 + \theta_3 x_3 (|x_1|^2 + |x_2|^2 + |x_3|^2) \\ \theta_3 x_2 x_3 x_1^* \\ 0 \\ \theta_3 x_3^2 x_2^* \\ \theta_3 x_3^2 x_1^* \\ \theta_3 x_1^2 x_3^* \\ \theta_3 x_1 x_2 x_3^* \\ \theta_3 x_2^2 x_3^* \\ \theta_3 x_1^2 x_2^* \end{bmatrix}. \tag{14}$$

instead of (12). Comparing to Figure 2, these computation steps have processed the data $x_1, ..., x_K$ through precoding in the virtual array domain, through DPDs and through an inverse Fourier transform. Since $L_\mathrm{v} < L$, fewer DPD computations have been performed whilst generating the same predistorted data streams as in (12). And since these data streams are separated, they can then easily be combined or precoded to an arbitrarily large physical array of size $L \geq L_\mathrm{v}$ by merely adding zeros and rearranging the terms.

By combinatorial trials, i.e. computing (13) for all possible combinations of $\{b_1, b_2, b_3\}$, $L_\mathrm{v} = 13$ is found to be the smallest virtual domain that for any L produces all main and intermodulation streams separated as in (14) for $K = 3$, $P = 3$. Similarly, $L_\mathrm{v} = 4$ is the smallest such virtual domain for $K = 2$ users, and $L_\mathrm{v} = 30$ for $K = 4$. However, there are cases when the virtual domain can be made with an even smaller L_v, without loss of information. This will be explained further in the following subsection.

4.2. Special Beam Configuration Cases

Denote $\{b'_1, b'_2, b'_3\}$ as the set of main beam indices in the virtual domain, with $\{b_1, b_2, b_3\}$ corresponding to the actual user directions. Depending on $\{b_1, b_2, b_3\}$ and L, different choices of $\{b'_1, b'_2, b'_3\}$ and L_v can be made to yield an optimal virtual array. More exact details on the problem of finding a virtual subspace is found in Appendix A, and is detailed statistically in the results of Section 5.3. The key phenomena explaining why this can occur is the array aliasing, as observed in Subsection 3.2, which can cause intermodulation terms to overlap. For example, evenly spaced beams in an even length array produces IM terms only at even beam indices. Concretely, say $L = 16$ and $\{b_1, b_2, b_3\} = \{2, 4, 6\}$. Then, by (13), the beam indices for a third order nonlinearity are $[2, 4, 6, 8, 10, 14, 16]$, a total of seven unique beam directions. However, computing (13) with $L_v = 7$ it can be noted that with $\{b'_1, b'_2, b'_3\} = \{1, 2, 3\}$ the same IM terms will overlap with one another, but at indices $[1, 2, 3, 4, 5, 6, 7]$. This is illustrated for the main beams and one IM beam in Figure 3(**a**) and Figure 3(**b**). Figure 3(**c**) showcases how it can alternatively be obtained for $L_\mathrm{v} = 13$ by first generating all IM terms at unique indices, before moving them to the appropriate overlap index. Thus, the virtual domain size can be made smaller in special cases. The resulting virtual domain sizes in the proposed approach are as such at worst of similar size as the cardinality of unique main beam and IM beam directions.

© 2025 by the author(s). Distributed under a Creative Commons CC BY license.

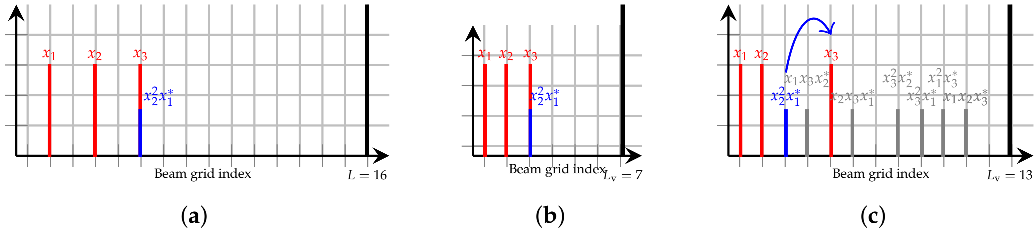

Figure 3. Beam occurrences for $\{b_1, b_2, b_3\} = \{2, 4, 6\}$ in real and virtual arrays, with placement of $x_2^2x_1^*$ highlighted. (**a**) Beam occurrences in real array. (**b**) Beam occurrences when $L_v = 7$, $\{b'_1, b'_2, b'_3\} = \{1, 2, 3\}$. (**c**) Beam occurrences when $L_v = 13$, $\{b'_1, b'_2, b'_3\} = \{1, 2, 5\}$.

4.3. Non-DFT Beamforming

For analytical purposes, this work has focused on LOS channels, wherein the columns of the DFT precoder matrix of (9) describes the inverse channel for transmission in those orthogonal LOS directions. However, more generally, if the wireless channel model can be accurately described with

$$\boldsymbol{Y} = \boldsymbol{H} f_{\mathrm{PA}}(\boldsymbol{z}) \,, \tag{15}$$

then the method is still applicable with some modification. Looking at the bar plots in Figure 2, and exemplified in (14), it is seen that the main and IMD beam components are separated after the IFFT. Thus, the final block can be replaced with a different precoding matrix $\boldsymbol{W}$. Presume for example that some general beamforming vector $\boldsymbol{w}^{(1)}$ should be applied to spatially direct x_1, and $\boldsymbol{w}^{(2)}$ to spatially direct x_2. Seen exemplified in (5), the third order off-beam beamforming vectors will then be $\left(\boldsymbol{w}^{(1)}\right)^2\left(\boldsymbol{w}^{(2)}\right)^*$ and $\left(\boldsymbol{w}^{(2)}\right)^2\left(\boldsymbol{w}^{(1)}\right)^*$, for $x_1^2x_2^*$ and $x_2^2x_1^*$, respectively. Thus, the precoder in the final block could be computed with $\boldsymbol{W} = \left[\, \boldsymbol{w}^{(1)} \;\; \boldsymbol{w}^{(2)} \;\; \left(\boldsymbol{w}^{(1)}\right)^2\left(\boldsymbol{w}^{(2)}\right)^* \;\; \left(\boldsymbol{w}^{(2)}\right)^2\left(\boldsymbol{w}^{(1)}\right)^* \,\right]$ instead of through an FFT. A simple simulation case is shown in Section 5.5, with more complex cases left for future work.

4.4. Generalization to Higher Order Terms

The analysis so far has considered third order IM beams. Extension to higher orders is very possible, by letting (4) include higher order terms and redoing the computations from there. This will give rise to e.g. 5th order IM terms such as $x_3^3x_1^*x_2^*$, with corresponding beam index $\overline{3b_3 - b_1 - b_2}$. As previously, some of the IM terms are always directed towards the users, and some are off-beams. Considering all these possible IM beams, the beam domain is only sparse for large L, and for VA-DPD to guarantee complete equivalence to PP-DPD for any beam configuration, L_v must be increased accordingly. However, the fifth order IM terms will typically have significantly lower power than the first and third order terms. Thus, they can often be neglected in off-beam directions.

4.5. Analogy with Frequency Relocation

Whilst not a direct counterpart, the proposed VA-DPD approach has, as previously mentioned, similarities to e.g. frequency relocation [11]. Namely, a signal that is sparse in one of its domains is densified in that domain, prior to DPD processing. Figure 4(a) shows how a multi-band signal, sparse in the frequency domain, is relocated to have frequency components closer to one another, where one when then performs DPD computations. Figure 4(b) in contrast shows an original, sparse beam domain compared to its densified virtual beam space, where DPD processing is performed. However, a challenge in multi-band frequency relocation is when bands are unevenly spaced, giving rise to IM products that end up at new frequency locations. In such cases, in [11], uniform downsampling whilst maintaining the relative spacing of bands is performed. This, however, will often not densify the frequency spectrum to only contain the relevant bands and IM products. In contrast, VA-DPD can in the multi-beam setting achieve a greater degree of dimensionality reduction by careful choice of the relocated beam indices in the virtual domain.

© 2025 by the author(s). Distributed under a Creative Commons CC BY license.

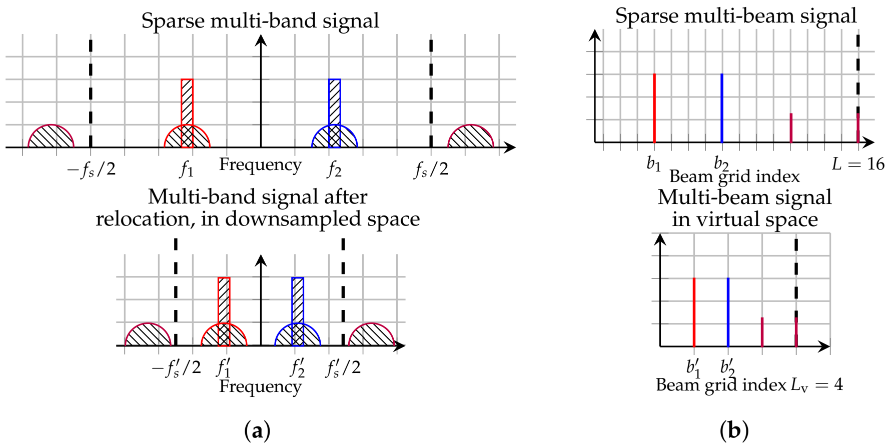

Figure 4. Comparison of a multi-band frequency relocation approach for densifying the frequency spectrum, to the virtual array approach for densifying the beam domain. (**a**) Power spectral density of a multi-band signal passed through a nonlinearity, with induced IMDs, in the frequency domain. (**b**) Power of a multi-beam signal passed through a nonlinearity, with induced IMDs, in beam domain.

5. Numerical Setup and Results

For the numerical simulations, a setup with $L = 28$ or 64, depending on the subsection, antennas in a uniform, linear array serving $K = 2$ or 3 users is considered. Each PA is modelled with a baseband Saleh model [17], equal on each PA branch, with added Gaussian noise $\boldsymbol{n}_l$ at the output as

$$f_{\mathrm{PA},l}(\boldsymbol{z}_l) = \frac{a\boldsymbol{z}_l}{1 + b|\boldsymbol{z}_l|^2} + \boldsymbol{n}_l\,, \tag{16}$$

with $a = 1, b = 0.47$. The desired signal is set to

$$\boldsymbol{Y}_\mathrm{d} = a_d \boldsymbol{H}\boldsymbol{z}\,, \tag{17}$$

with $a_d = 0.95$. The noise power of $\boldsymbol{n}_l$ is chosen to give signal-to-noise ratios between 50-60 dB. $\boldsymbol{H}$ is chosen as a LOS channel, from L branches to $Q = 181$ evenly spaced observation directions in the azimuth plane. The baseband user data streams are generated through bandlimiting complex Gaussian noise to a bandwidth of 30 MHz, and normalized to a root-mean square value of 0.13, with peak-to-average power ratio about 8.3 dB. For each user stream, $N = 65536$ baseband samples are generated.

Four linearization cases are simulated per transmit configuration. Not using DPD (No DPD), using per-PA (PP) DPD, using beam-domain (BD) DPD based on [5,6], and using virtual-array (VA) DPD.

5.1. DPD Identification

With this setup, conventional iterative learning control (ILC) [18] is modified with a simple extension and used to find the optimal input signals $\boldsymbol{z}_l$ to each PA in the array. Denote

$$\boldsymbol{z}^{[i]} = \begin{bmatrix} \boldsymbol{z}_1^{[i]} \\ \vdots \\ \boldsymbol{z}_L^{[i]} \end{bmatrix}, \tag{18}$$

as the DPD input at iteration $[i]$. Then the DPD input at iteration $[i+1]$, $\boldsymbol{z}^{[i+1]}$, based on the OTA measured $\boldsymbol{Y}^{[i]}$ and desired signal $\boldsymbol{Y}_\mathrm{d}$, is found as

$$\boldsymbol{z}^{[i+1]} \leftarrow \boldsymbol{z}^{[i]} + \eta \boldsymbol{H}^\dagger (\boldsymbol{Y}_\mathrm{d} - \boldsymbol{Y}^{[i]})\,, \tag{19}$$

Here, η is a step parameter for the iterations, and $\boldsymbol{H}^\dagger = (\boldsymbol{H}^*\boldsymbol{H})^{-1}\boldsymbol{H}^*$ is the pseudoinverse of the channel matrix $\boldsymbol{H}$. This procedure is suitable to perform offline as an initial identification, whilst online

© 2025 by the author(s). Distributed under a Creative Commons CC BY license.

Preprints.org (www.preprints.org) | NOT PEER-REVIEWED | Posted: 9 February 2026 doi:10.20944/preprints202602.0713.v1

adaptation of DPD coefficients can be done with other known methods. The signals $\boldsymbol{z}_l$ are after ILC convergence shifted to the virtual domain, yielding target signals $z_l^{'}$, as in Figure 2. The shifting is performed by doing the VA processing steps in reverse. That is, an IFFT is performed on $\boldsymbol{z}$ along the branches, followed by that the streams of different considered beams from $\boldsymbol{z}$ are relocated to their VA-placement $\{b_1', ..., b_B'\}$, whilst removing streams that were zero-padded in the forward path. Lastly, an FFT is done in the virtual domain to go from the virtual beam domain to the virtual antenna domain, and obtain $z_l^{'}$. Forming a nonlinear model from u_l' to z_l' in the virtual domain through polynomial DPD models yields a predistorted virtual domain signal and basis

$$\boldsymbol{z}_l' = \boldsymbol{F}_{u_l'}\boldsymbol{\theta}_l \, , \boldsymbol{F}_{u_l'} = \left[\, u_l',\, u_l'|u_l'|^2,\, ...u_l'|u_l'|^{P-1} \,\right] \tag{20}$$

where DPD coefficients are obtained as

$$\boldsymbol{\theta}_l = \boldsymbol{F}_{u_l'}^{\dagger} z_l' \, . \tag{21}$$

For conventional PP-DPD, equations (20), (21) are used but for the setup as in Figure 1, with target signals $\boldsymbol{z}_l$ and inputs $\boldsymbol{u}_l$, $l = 1, ..., L$. For BD-DPD, each unique bases expressed in terms of $x_1, ..., x_K$, obtainable from the expansion of $\sum_{p=0,2,...}^{P-1} z_l|z_l|^p$, is used. This includes offbeams as in Table 1, fifth order terms as in Table 2, and main beam terms such as $x_1|x_1|^2, x_2|x_3|^2$.

Table 2. Fifth order IM terms for static non-linearity of order $P = 5$, with $K = 2, 3$ concurrent users.

Number of users	Fifth order terms	Total number of fifth order terms
$K = 2$	$x_1|x_1|^4, x_1|x_2|^4, x_1|x_1|^2|x_2|^2$ $x_2|x_2|^4, x_2|x_1|^4, x_2|x_1|^2|x_2|^2$ $x_1^3(x_2^*)^2, x_2^3(x_1^*)^2$ $x_1|x_1|^2x_2^2, x_2|x_2|^2x_1^2$ $x_1^2|x_1|^2x_2^*, x_2^2|x_2|^2x_1^*$	12
$K = 3$	$x_1|x_1|^4, ... , x_1|x_2|^2|x_3|^2$	60

5.2. Tri-Beam Scenario

In Figure 5, a concurrent tri-beam scenario is shown. For this scenario there are $L = 64$ transmit branches, with beams in beam directions $\{b_1, b_2, b_3\} = \{7, 23, 49\}$. In Figure 5(**a**) and Figure 5(**b**), the power of the desired signal Y_d, over different angles, is visualized in contrast to the distortion power remaining after applying no DPD, PP-DPD, BD-DPD and the proposed VA-DPD approach with either odd order $P = 3$ or $P = 5$ DPDs. For VA-DPD, the virtual array uses $L_\text{v} = 13$ branches, meaning it can capture third order beam direction information without loss. Consequently, Figure 5(**a**), highlights how VA-DPD is equivalent in performance to PP-DPD and BD-DPD for a DPD of order $P = 3$. This is seen from that the yellow line, corresponding to PP-DPD distortion, is precisely covered by the purple and green, of VA-DPD and BD-DPD, respectively. On the other hand, compared to Figure 5(**b**), Figure 5(**b**) shows that if applying fifth order DPDs whilst only considering up to third order terms in the virtual array dimensioning, the distortion power in the user directions is reduced equivalently to PP-DPD and BD-DPD, by an additional 5 dB compared to $P = 3$. However, the off-beam linearization performance is not improved correspondingly, as seen by the residual distortion e.g. around angles 28-35°.

© 2025 by the author(s). Distributed under a Creative Commons CC BY license.

 doi:10.20944/preprints202602.0713.v1

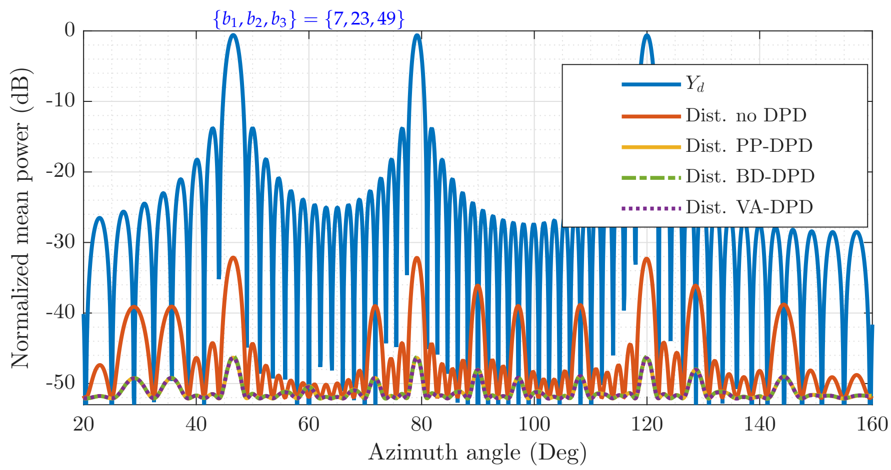

(a)

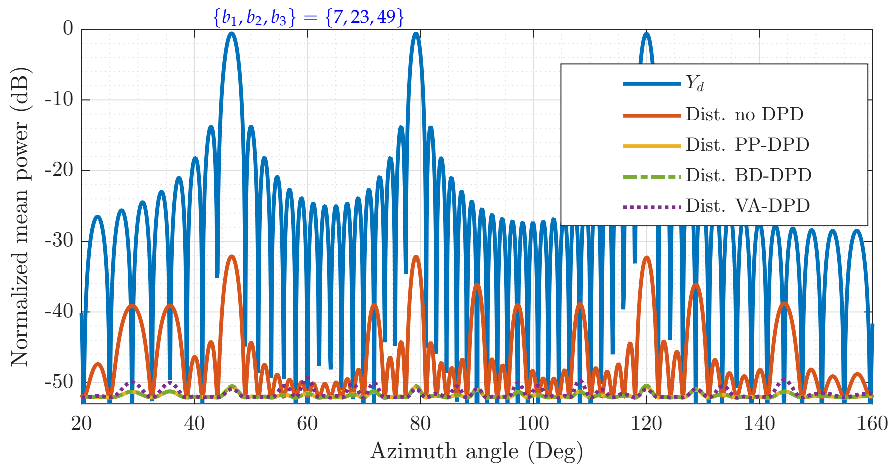

(b)

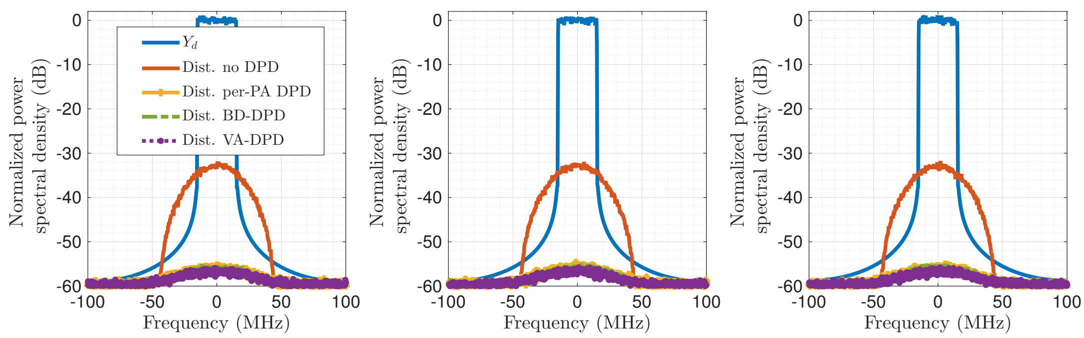

(c)

Figure 5. Normalized power of the desired signal Y_d shown in comparison to the distortion power remaining after no DPD, per-PA (PP) DPD, the proposed virtual array (VA) DPD and beam domain (BD) DPD, for concurrent tri-beam transmission. DPDs include odd order terms up to, and including, order P. (**a**) Mean power in varying spatial directions, $P = 3$. (**b**) Mean power in varying spatial directions, $P = 5$. (**c**) Power spectral density in user directions, $P = 5$.

With only $L_v = 13$ branches and a first, third plus fifth order term per branch for linearization, only $13 \cdot 3 = 39$ one-dimensional DPD multiplications are needed. Alternatively, $L_v = 13$ 1D-LUT look-ups are done to find the appropriate predistorted values per sample. In contrast, PP-DPD requires $64 \cdot 3$ DPD multiplications, or 64 1D-LUT look-ups. Thus, complexity is reduced by $100 \cdot |13 - 64| / 64 \approx 80\%$ in VA-DPD compared to PP-DPD. Lastly, seen from Table 1 and Table 2, BD-DPD needs to account for 3 linear, 12 third order and 60 fifth order terms. For a LUT implementation, each of the twelve unique data streams, going in different spatial directions, needs a three-dimensional table look-up.

© 2025 by the author(s). Distributed under a Creative Commons CC BY license.

Preprints.org (www.preprints.org) | NOT PEER-REVIEWED | Posted: 9 February 2026 doi:10.20944/preprints202602.0713.v1

5.3. Virtual Array Dimensioning

The results of this section describe how small the virtual array can be dimensioned in terms of L_v, to account for all IM beams, with respect to special cases as described in Subsection 4.2. In Figure 6 the proportion of beam configuration $\{b_1, b_2, b_3\}$ that can be represented with a virtual array of length L_v is shown for varying arrays sizes $L = 16$, 32, 64, and in Table 3 and Table 4, it is shown for various L, and $P = 3, 5$. Most noticeably, the proportion of cases requiring a larger L_v increases with L. This correlates to that in a larger beam space, the IM products end up in unique beam directions more often. The results highlight that there are cases when the beam domain is especially sparse, such that the VA-DPD can be performed at an even lower computational complexity.

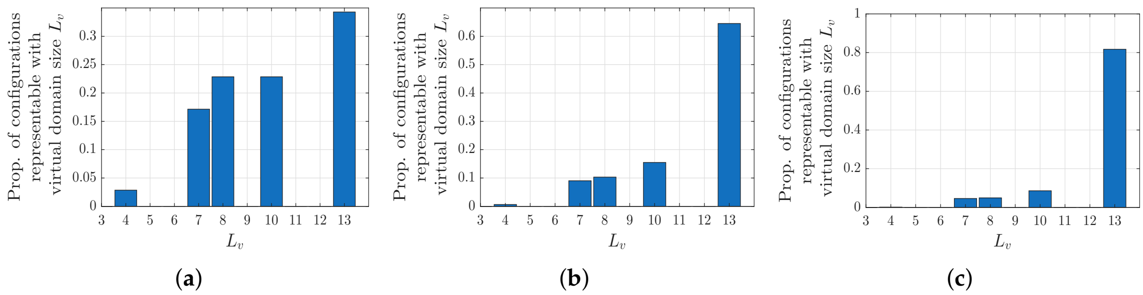

Figure 6. Proportion of main beam configuration cases in the original domain of size L that can be represented by a virtual domain of size L_v, considering IM terms of order $P = 3$. (**a**) Array size $L = 16$. (**b**) Array size $L = 32$. (**c**) Array size $L = 64$.

Table 3. Percentage (%) of main beam configurations in the original domain of size L that can be represented by a virtual domain of size L_v, for IM terms of order $P = 3$.

L \ L_v	**3**	**4**	**5**	**6**	**7**	**8**	**9**	**10**	**12**	**13**
20	0	2	4	0	11	14	0	21	0	49
24	< 1	1	0	4	10	12	0	14	21	38
30	< 1	0	2	2	7	9	0	15	18	47
36	< 1	1	0	2	7	7	3	11	12	58
130	0	0	$\ll 1$	0	2	2	0	5	0	91
256	0	$\ll 1$	0	0	1	1	0	2	0	95

Table 4. Percentage (%) of main beam configurations in the original domain of size L that can be represented by a virtual domain of size L_v, for IM terms of order $P = 5$.

L \ L_v	**4**	**8**	**11**	**12**	**16**	**21**	**22**	**24**	**26**	**30**
32	1	4	8	8	23	10	5	21	10	10
64	< 1	1	4	4	10	7	4	15	7	47
128	$\ll 1$	< 1	2	2	5	4	2	8	4	71

5.4. Power Amplifier Variations

It was noted earlier that BD-DPD assumes equal PAs across branches. It is this assumption that mathematically allows for a common DPD to be used prior to the precoder in BD-DPD, without losing any ability to linearize the system [6]. This assumption is not quite as rigidly held in the proposed VA-DPD, as DPD variations across the virtual array branches can be adapted. As such, to investigate whether or not VA-DPD might handle PA variations better in comparison to BD-DPD, the PA model is changed to

$$f_{\mathrm{PA},l}(x) = c_{1,l}x + c_{3,l}x|x|^2 , \tag{22}$$

© 2025 by the author(s). Distributed under a Creative Commons CC BY license.

to easier represent gain and phase variations in the nonlinear PA response relative to the linear response, variations which can not be compensated by calibration. The first order coefficients are set to $c_{1,l} = 1$ for all branches, whilst $c_{3,l}$ are varied from a nominal value of -0.55 with magnitude standard deviation 0.028 and random phases from a uniform distribution between $[-20, 20]°$. Figure 7 showcases a tri-beam case with $\{b_1, b_2, b_3\} = \{1, 3, 10\}$, $L = 16$, $L_v = 7$. In Figure 7(**a**) and Figure 7(**c**), the PAs exhibit no variations, whilst in Figure 7(**b**) and Figure 7(**d**) they do. Notably, both VA-DPD and BD-DPD deteriorate in performance relative to PP-DPD with PA variations. However, VA-DPD reduces distortion more than BD-DPD in all user directions. This because whilst BD-DPD adapts one set of coefficients, prior to the precoder, to hold for linearization across all branches, VA-DPD can have some DPD coefficient variations with $l = 1, ..., L_v$.

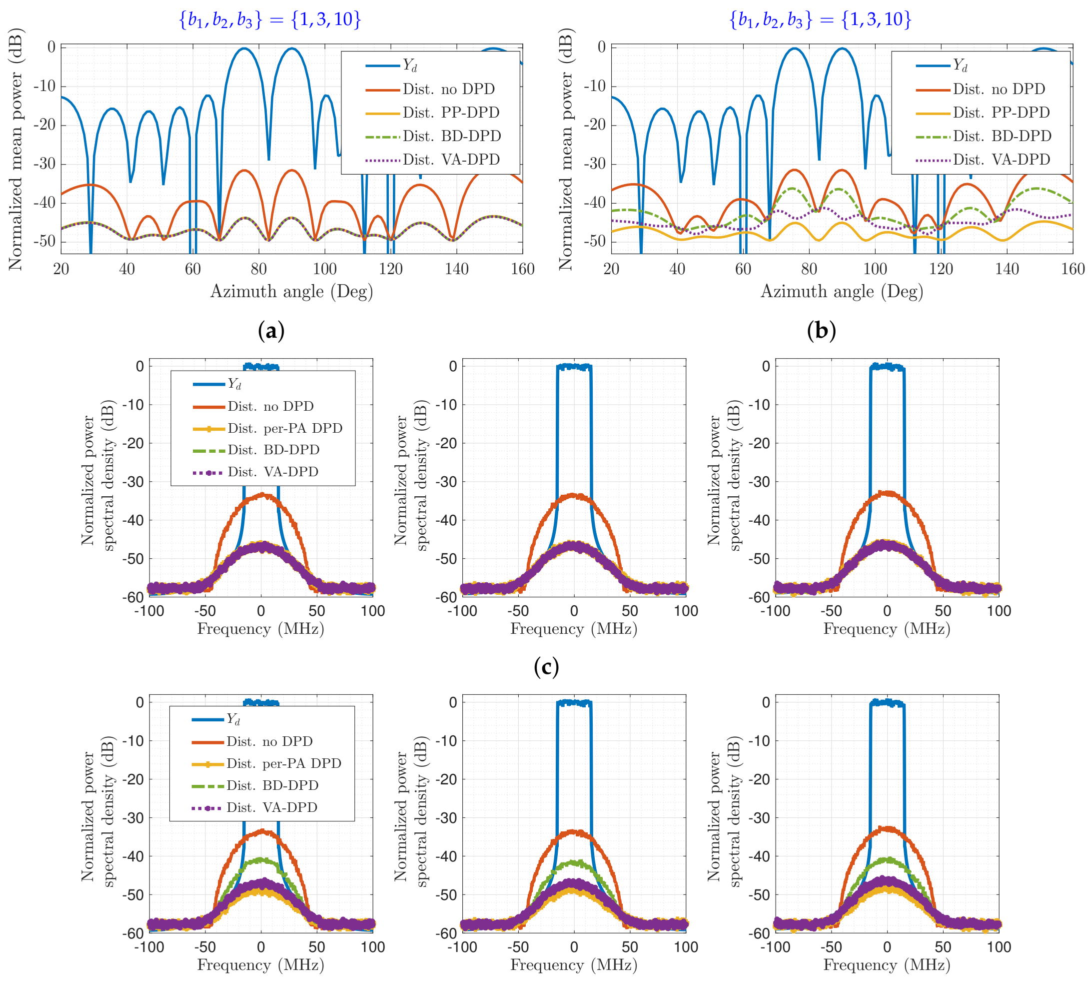

Figure 7. Normalized power of the desired signal Y_d shown in comparison to the distortion power remaining after no DPD, Per-PA (PP) DPD, the proposed virtual array (VA) DPD and beam domain (BD) DPD, for concurrent tri-beam transmission, with or without PA variations. DPDs include first and third order terms. (**a**) Mean power in varying spatial directions. No PA variations. (**b**) Mean power in varying spatial directions. PA variations. (**c**) Power spectral density in user directions. No PA variations. (**d**) Power spectral density in user directions. PA variations.

5.5. Non-FFT Precoder

In Figure 8, a two-user scenario for a random channel $\boldsymbol{H}$ of dimension $L \times Q$ consisting of complex Gaussian number distributed as $\mathcal{CN}(0, 1)$ is shown, with users in directions $[71, 106]°$. The array is of size $L = 28$, and virtual array of size $L_v = 4$. Pre-coding vectors are chosen as the pseudo-inverse of the respective channel vectors, i.e. $\boldsymbol{w}_1 = \boldsymbol{H}_{71}^{\dagger}$, $\boldsymbol{w}_2 = \boldsymbol{H}_{106}^{\dagger}$. First to note, all linearization methods achieve about 20 dB improvement in distortion reduction. Secondly, neither the linear power nor the

© 2025 by the author(s). Distributed under a Creative Commons CC BY license.

Preprints.org (www.preprints.org) | NOT PEER-REVIEWED | Posted: 9 February 2026 doi:10.20944/preprints202602.0713.v1

residual distortion form clear beam directions, but are instead spread across the spatial range, due to the randomness of the channel. A $100 \cdot |4 - 28|/28 \approx 86\%$ reduction in DPD complexity is achieved for VA-DPD compared to PP-DPD.

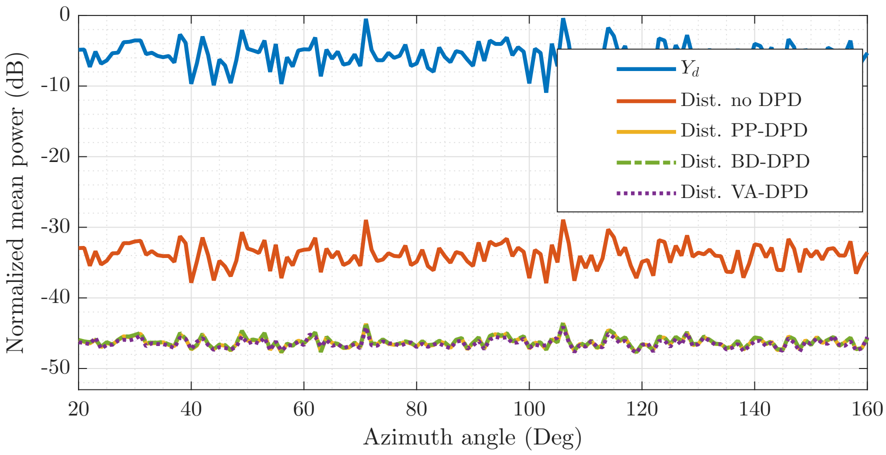

(**a**)

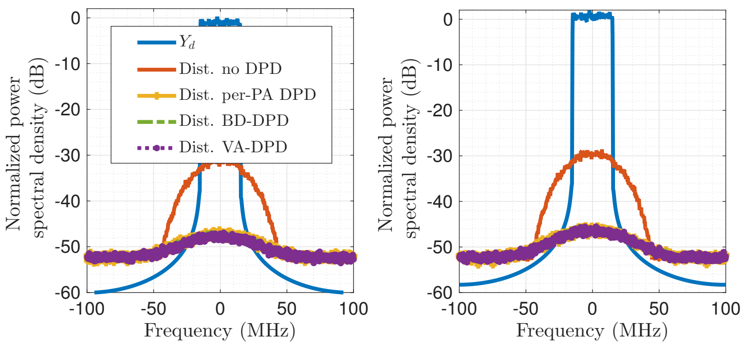

(**b**)

Figure 8. Normalized power of the desired signal Y_d shown in comparison to the distortion power remaining after no DPD, per-PA (PP) DPD, the proposed virtual array (VA) DPD and beam domain (BD) DPD, for concurrent dual-beam transmission in random channel. $P = 7$ is used for the DPDs. (**a**) Mean power in varying spatial directions. No PA variations. (**b**) Power spectral density in user directions.

6. Conclusion

The proposed DPD schematic, using FFT beamforming and virtual array DPD processing, is shown capable of reducing DPD complexity manyfold in contrast to conventional per-PA DPD, when many transmit branches serve few users. The virtual array DPD scheme is shown operable for varying degrees of PA nonlinearities, and for different channel conditions and multi-user scenarios. In contrast to previous approaches utilizing a beam-domain framework, the proposed approach utilizes single-input, single-output DPD units that are computationally cheap to implement. Overall, the approach offers a flexible and powerful alternative to multi-user linearization for large MIMO arrays with digital beamforming.

Author Contributions: The contributions from different authors of this work are as follows. Conceptualization, Björn Langborn and Rui Hou; Implementation, Björn Langborn; Technical refinement and generalization, all authors; Writing, Björn Langborn; Review and editing, all authors; Funding acquisition, Thomas Eriksson, Christian Fager and Rui Hou.

Funding: This work was supported by Vinnova, Formas and the Swedish Energy Agency within the strategic innovation programme 'Smartare Elektroniksystem', and by Chalmers University of Technology and Ericsson AB.

© 2025 by the author(s). Distributed under a Creative Commons CC BY license.

Preprints.org (www.preprints.org) | NOT PEER-REVIEWED | Posted: 9 February 2026 doi:10.20944/preprints202602.0713.v1

Data Availability Statement: Data generated in this work, described in Section 5, can reproduced with the MATLAB function randn.

Conflicts of Interest: The authors declare no conflicts of interest.

Appendix A. Finding a Virtual DPD Space

Finding a virtual array representation for a given array of size L transmitting beams $b_1, \ldots, b_K$ involves finding an appropriate virtual array size L_v and virtual beam placement $b'_1, \ldots, b'_K$. In the original antenna domain, for a tri-beam case, main and intermodulation beams will end up on integer indices $c_1, \ldots, c_{12}$, as in

$$\begin{aligned}
b_1 &= c_1 \\
b_2 &= c_2 \\
b_3 &= c_3 \\
(2b_1 - b_2) - L\left\lfloor \frac{2b_1 - b_2 - 1/2}{L} \right\rfloor &= c_4 \\
&\vdots \\
(b_2 + b_3 - b_1) - L\left\lfloor \frac{b_2 + b_3 - b_1 - 1/2}{L} \right\rfloor &= c_{12}\,,
\end{aligned} \tag{A1}$$

where $\{c_1, \ldots, c_{12}\} \in [1, L]$. The set $\{c_1, \ldots, c_{12}\}$ might not be a unique set of 12 integers. This can be exemplified with beams $\{b_1, b_2, b_3\} = \{1, 2, 4\}$, $L = 16$ where the off-beam indices are $\{16, 3, 14, 7, 16, 6, 15, 3, 5\}$ such that (A1) becomes

$$\begin{aligned}
b_1 &= c_1 = 1 \\
b_2 &= c_2 = 2 \\
b_3 &= c_3 = 4 \\
(2b_1 - b_2) - L\left\lfloor \frac{2b_1 - b_2 - 1/2}{L} \right\rfloor &= c_4 = c_8 = 16 \\
(2b_2 - b_1) - L\left\lfloor \frac{2b_2 - b_1 - 1/2}{L} \right\rfloor &= c_5 = c_{11} = 3 \\
&\vdots \\
(b_1 + b_3 - b_2) - L\left\lfloor \frac{b_1 + b_3 - b_2 - 1/2}{L} \right\rfloor &= c_{11} = c_5 = 3 \\
(b_2 + b_3 - b_1) - L\left\lfloor \frac{b_2 + b_3 - b_1 - 1/2}{L} \right\rfloor &= c_{12} = 5\,,
\end{aligned} \tag{A2}$$

© 2025 by the author(s). Distributed under a Creative Commons CC BY license.

Preprints.org (www.preprints.org) | NOT PEER-REVIEWED | Posted: 9 February 2026 doi:10.20944/preprints202602.0713.v1

The objective is then to find a virtual subspace with L_v, b'_1, b'_2, b'_3 such that

$$\begin{aligned}
b'_1 &= c'_1 \\
b'_2 &= c'_2 \\
b'_3 &= c'_3 \\
(2b'_1 - b'_2) - L_v \left\lfloor \frac{2b'_1 - b'_2}{L_v} \right\rfloor &= c'_4 = c'_8 \\
(2b'_2 - b'_1) - L_v \left\lfloor \frac{2b'_2 - b'_1}{L_v} \right\rfloor &= c'_5 = c'_{11} \\
&\vdots \\
(b'_1 + b'_3 - b'_2) - L_v \left\lfloor \frac{b'_1 + b'_3 - b'_2}{L_v} \right\rfloor &= c'_{11} = c'_5 \\
(b'_2 + b'_3 - b'_1) - L_v \left\lfloor \frac{b'_2 + b'_3 - b'_1}{L_v} \right\rfloor &= c'_{12},
\end{aligned} \tag{A3}$$

for any $\{c'_1, ..., c'_{12}\} \in [1, L_v]$. This is a Diophantine system of equations, and generally not trivial to solve. However, in practice, it can be solved for offline, and the indices obtained during runtime using a lookup table. In this work, the pseudo-algorithm of Algorithm A1 describes one approach to solving the systems of equations, for a general case with arbitrary number of beams K and branches L. Depending on K, heuristic knowledge can limit the search space Lvs and mbs in Algorithm A1. One general constraint is $L_v \geq |\{b'_1, b'_2, ..., b'_2 + b'_3 - b'_1\}|$, i.e. the virtual domain size can never be reduced below the cardinality of the set it is supposed to represent.

Algorithm A1 Algorithm to find virtual space representation.

```
Require: mb, L // Main beam indices mb and array size L
  // Get off-beams, and cardinality of full index set
  ob = get_offbeams(mb,L)
  ab = [mb ob]
  c = length(unique(ab))
  // Try virtual subspace size Lv out of candidates Lvs
  for Lv=Lvs do
    // Try virtual main beams mbv out of candidates mbvs
    for mbv=mbvs do
      // Get off-beam indices for mbv
      obv = get_offbeams(mbv,Lv)
      abv = [mbv obv]
      // Relabel ab and abv such that the first element, and
      all other elements in the vector with same value,
      is labelled 1. Do correspondingly for the remaining elements.
      Obtain ab_relabel, abv_relabel
      if ab_relabel==abv_relabel then
        // Virtual array representation {mbv,Lv} found.
      end if
    end for
  end for
```

References

1. Kakkavas, A.; Seco-Granados, G.; Wymeersch, H.; Garcia, M.H.C.; Stirling-Gallacher, R.A.; Nossek, J.A. 5G Downlink Multi-Beam Signal Design for LOS Positioning. In Proceedings of the IEEE Global Communications Conference. IEEE, 2019. https://doi.org/10.1109/GLOBECOM38437.2019.9013374.

© 2025 by the author(s). Distributed under a Creative Commons CC BY license.

Preprints.org (www.preprints.org) | NOT PEER-REVIEWED | Posted: 9 February 2026 doi:10.20944/preprints202602.0713.v1

2. Liu, X.; Chen, W.; Chu, J.; Ghannouchi, F.M.; Feng, Z. Multi-Stream Spatial Digital Predistortion for Fully-Connected Hybrid Beamforming Massive MIMO Transmitters. *IEEE Transactions on Circuits and Systems I: Regular Papers* **2021**, *68*, 2998–3011. https://doi.org/10.1109/TCSI.2021.3072591.
3. Jing, J.; Yu, C. Multibeam Digital Predistortion for Millimeter-Wave Analog Beamforming Transmitters. *IEEE Microwave and Wireless Components Letters* **2020**, *30*, 209–212. https://doi.org/10.1109/LMWC.2019.2959431.
4. Yu, C.; Jing, J.; Shao, H.; Jiang, Z.H.; Yan, P.; Zhu, X.W.; Hong, W.; Zhu, A. Full-Angle Digital Predistortion of 5G Millimeter-Wave Massive MIMO Transmitters. *IEEE Transactions on Microwave Theory and Techniques* **2019**, *67*, 2847–2860. https://doi.org/10.1109/TMTT.2019.2918450.
5. Brihuega, A.; Anttila, L.; Valkama, M. Beam-Level Frequency-Domain Digital Predistortion for OFDM Massive MIMO Transmitters. *IEEE Transactions on Microwave Theory and Techniques* **2023**, *71*, 1412–1427. https://doi.org/10.1109/TMTT.2022.3222320.
6. Braithwaite, R.N. Amplifier Nonlinearities in an Antenna Array During Spatially-Multiplexed Transmissions. In Proceedings of the IEEE Radio and Wireless Symposium. IEEE, 2020, pp. 235–238. https://doi.org/10.1109/RWS45077.2020.9050029.
7. Bassam, S.A.; Helaoui, M.H.; Ghannouchi, F.M. 2-D digital predistortion (2-D-DPD) architecture for concurrent dual-band transmitters. *IEEE Transactions on Microwave Theory and Techniques* **2011**, *59*, 2547–2553. https://doi.org/10.1109/TMTT.2011.2163802.
8. Liu, Y.J.; Chen, W.; Zhou, J.; Zhou, B.H.; Ghannouchi, F.M. Digital predistortion for concurrent dual-band transmitters using 2-D modified memory polynomials. *IEEE Transactions on Microwave Theory and Techniques* **2013**, *61*, 281–290. https://doi.org/10.1109/TMTT.2012.2228216.
9. Eriksson, T.; Fager, C. Digital predistortion of concurrent multiband communication systems. In Proceedings of the 2014 IEEE International Conference on Acoustics, Speech and Signal Processing (ICASSP). IEEE, 5 2014, pp. 3918–3922. https://doi.org/10.1109/ICASSP.2014.6854336.
10. Younes, M.; Kwan, A.; Rawat, M.; Ghannouchi, F.M. Three-Dimensional digital predistorter for concurrent tri-band power amplifier linearization. In Proceedings of the IEEE MTT-S International Microwave Symposium Digest (MTT). IEEE, 2013, pp. 1–4. https://doi.org/10.1109/MWSYM.2013.6697635.
11. Yu, C.; Xia, J.; Zhu, X.W.; Zhu, A. Single-Model Single-Feedback Digital Predistortion for Concurrent Multi-Band Wireless Transmitters. *IEEE Transactions on Microwave Theory and Techniques* **2015**, *63*, 2211–2224. https://doi.org/10.1109/TMTT.2015.2429633.
12. Kolomvakis, N.; Bavand, M.; Bahceci, I.; Gustavsson, U. A Distortion Nullforming Precoder in Massive MIMO Systems With Nonlinear Hardware. *IEEE Wireless Communications Letters* **2022**, *11*, 1775–1779. https://doi.org/10.1109/LWC.2022.3175147.
13. Mollen, C.; Gustavsson, U.; Eriksson, T.; Larsson, E.G. Spatial characteristics of distortion radiated from antenna arrays with transceiver nonlinearities. *IEEE Transactions on Wireless Communications* **2018**, *17*, 6663–6679. https://doi.org/10.1109/TWC.2018.2861872.
14. Jing, J.; Shao, H.; Yan, P.; Jiang, Z.H.; Yu, C. Digital Predistortion of Millimeter-Wave Multi-beam Transmitters with Digital Beam-forming Network. In Proceedings of the 2019 IEEE MTT-S International Wireless Symposium (IWS), 2019, pp. 1–3. https://doi.org/10.1109/IEEE-IWS.2019.8803986.
15. Molina, A.; Rajamani, K.; Azadet, K. Concurrent Dual-Band Digital Predistortion Using 2-D Lookup Tables with Bilinear Interpolation and Extrapolation: Direct Least Squares Coefficient Adaptation. *IEEE Transactions on Microwave Theory and Techniques* **2017**, *65*, 1381–1393. https://doi.org/10.1109/TMTT.2016.2634001.
16. Wang, S.; Cao, W.; Hou, R.; Eriksson, T. A Digital Predistortion for Concurrent Dual-Band Power Amplifier Linearization Based on Periodically Nonuniform Sampling Theory. *IEEE Transactions on Microwave Theory and Techniques* **2022**, *70*, 466–475. https://doi.org/10.1109/TMTT.2021.3119340.
17. Saleh, A. Frequency-Independent and Frequency-Dependent Nonlinear Models of TWT Amplifiers. *IEEE Transactions on Communications* **1981**, *29*, 1715–1720. https://doi.org/10.1109/TCOM.1981.1094911.
18. Chani-Cahuana, J.; Landin, P.N.; Fager, C.; Eriksson, T. Iterative Learning Control for RF Power Amplifier Linearization. *IEEE Transactions on Microwave Theory and Techniques* **2016**, *64*, 2778–2789. https://doi.org/10.1109/TMTT.2016.2588483.

Disclaimer/Publisher's Note: The statements, opinions and data contained in all publications are solely those of the individual author(s) and contributor(s) and not of MDPI and/or the editor(s). MDPI and/or the editor(s) disclaim responsibility for any injury to people or property resulting from any ideas, methods, instructions or products referred to in the content.

© 2025 by the author(s). Distributed under a Creative Commons CC BY license.